Available online at www.sciencedirect.com
ScienceDirect
Journal of Sound and Vibration 325 (2009) 161–173
JOURNAL OF SOUND AND VIBRATION
www.elsevier.com/locate/jsvi

A hybrid method for transient wave propagation in a multilayered solid

Jiayong Tian*, Zhoumin Xie

Institute of Crustal Dynamics, China Earthquake Administration, P.O. Box 2855, Beijing 100085, PR China

Received 23 April 2008; received in revised form 17 February 2009; accepted 28 February 2009
Handling Editor: L.G. Tham
Available online 14 April 2009

Abstract

We present a hybrid method for the evaluation of transient elastic-wave propagation in a multilayered solid, integrating reverberation matrix method with the theory of generalized rays. Adopting reverberation matrix formulation, Laplace–Fourier domain solutions of elastic waves in the multilayered solid are expanded into the sum of a series of generalized-ray group integrals. Each generalized-ray group integral containing Kth power of reverberation matrix $\mathbf{R}$ represents the set of K-times reflections and refractions of source waves arriving at receivers in the multilayered solid, which was computed by fast inverse Laplace transform (FILT) and fast Fourier transform (FFT) algorithms. However, the calculation burden and low precision of FILT–FFT algorithm limit the application of reverberation matrix method. In this paper, we expand each of generalized-ray group integrals into the sum of a series of generalized-ray integrals, each of which is accurately evaluated by Cagniard–De Hoop method in the theory of generalized ray. The numerical examples demonstrate that the proposed method makes it possible to calculate the early-time transient response in the complex multilayered-solid configuration efficiently.

1. Introduction

Transient elastic-wave propagation in a multilayered medium plays an important role in the fields of seismology, ocean acoustics, and non-destructive evaluation [1]. Extensive literatures have developed systematic methodology to evaluate the wave propagation in the multilayered solid. One of the most important matrix formulations is transfer matrix method developed first by Thomson [2] and then furthered by Haskell [3]. The simple configuration and efficient computational ability facilitate its wide application in many research fields. Stiffness matrix method [4,5] and global matrix method [6] have been proposed to resolve the inherent computational instability for large product of frequency and thickness in transfer matrix method. The stiffness matrix method utilizes the stiffness matrix of each sublayer in a recursive algorithm to obtain a stack stiffness matrix for the multilayered medium. The global matrix method involves a global banded matrix whose size grows with the number of the sublayers.

*Corresponding author. Tel./fax: +86 10 62913587.
E-mail address: chenlitedtian@yahoo.com.cn (J. Tian).

0022-460X/$ - see front matter
doi:10.1016/j.jsv.2009.02.041

Spencer [7] proposed the method of generalized rays to evaluate the transient wave propagation in the multilayered solid, which was originally developed for geophysical applications. In the theory of generalized rays, elastic waves propagating along various ray paths because of multiple reflections and refractions are expressed as a series of generalized-ray integrals, each of which can be evaluated accurately by Cagniard–De Hoop method [8]. Since the transient response of one generalized ray is exact up to the arrival time of the next generalized ray, only a finite number of generalized rays will be involved in the early-time solution. Because the number of generalized-ray integrals increases remarkably as the increase of the observation duration and the number of sublayers, the method of generalized ray is only most effective in the evaluation of the generalized rays that arrive early at a receiver in the simple multilayered-solid configuration.

Lee [9] and Ma [10,11] formulated a system of equations with a coefficient matrix for the investigation of the transient waves in a layered solid. They rearranged the coefficient matrix in the special form consisting of the diagonal, lower, and upper triangular parts and then expanded the inversion of the coefficient matrix into a power series, which correspond to the finite wave groups involving the multiple reflected or refracted waves with the same times of reflections or refractions. Su et al. presented another matrix formulation method—the reverberation matrix method, to investigate the transient elastic waves in isotropic and transversely layered solid [12,13], which was originally developed to investigate the transient elastic waves in frames [14]. Considering the local scattering relations at interfaces and the transfer relations in the sublayer, a reverberation matrix is introduced to formulate a system of equations. According to the times of reflections and refractions of generalized rays at interfaces, the system of equations in Laplace–Fourier domain is automatically represented as a series of generalized-ray group integrals. Each generalized-ray group integral containing Kth power of reverberation matrix $\mathbf{R}$ represents the set of K times reflections and refractions of source waves arriving at receivers in the multilayered solid, which is very suitable to automatic computer programming compared with the theory of generalized rays. However, at present, generalized-ray group integrals are numerically evaluated by fast inverse Laplace transform (FILT) and fast Fourier transform (FFT) [12,13]. With the larger calculation burden and the lower computation precision, FILT–FFT algorithm is difficult to accurately confirm the arrival time of elastic waves, which makes it impossible to truncate the generalized-ray group integrals accurately. Furthermore, for the long-time responses, the FILT–FFT results will trend unstable, which limits the wide application of reverberation matrix method [15].

In order to calculate the generalized-ray group integrals efficiently, we build a clear connection between the generalized-ray group integrals and the generalized-ray integrals in this paper. Extracting phase functions from reverberation matrix and receiver matrix, each of generalized-ray group integrals can be further expanded into the sum of a series of the generalized-ray integrals, which can be accurately evaluated by Cagniard–De Hoop scheme in the theory of generalized rays. First, we briefly introduce reverberation matrix formulation for the evaluation of elastic-wave propagation in the multilayered solid. Second, we present an expansion method of the generalized-ray group integrals into the generalized-ray integrals. Lastly, we show two examples to validate the efficiency of the proposed method.

2. Reverberation matrix formulation

To simplify the analysis, we only consider in-plane wave propagation in an isotropic multilayered semi-infinite solid. In the multilayered solid containing $(N-1)$ sublayers overlaying on a semi-infinite solid shown in Fig. 1, the interfaces between sublayers are expressed by capital letters $I, J, \ldots$. Each sublayer is represented by its interfaces, for example sublayer IJ, sublayer $JK, \ldots$. As shown in Fig. 2, two local Cartesian coordinate systems $(x, y)^{IJ}$ and $(x, y)^{JI}$ are constructed at two interfaces of sublayer IJ, respectively. The thickness of the sublayer is represented by h^{IJ}.

The one-side Laplace transform with respect to time t and the double-side Laplace transform with respect to the spatial coordinate x are defined as

$$\hat{f}(\eta, y, p) = \int_{-\infty}^{\infty} \mathrm{e}^{-p\eta x} \int_{0}^{\infty} f(x, y, t)\mathrm{e}^{-pt}\,\mathrm{d}t\,\mathrm{d}x. \tag{1}$$

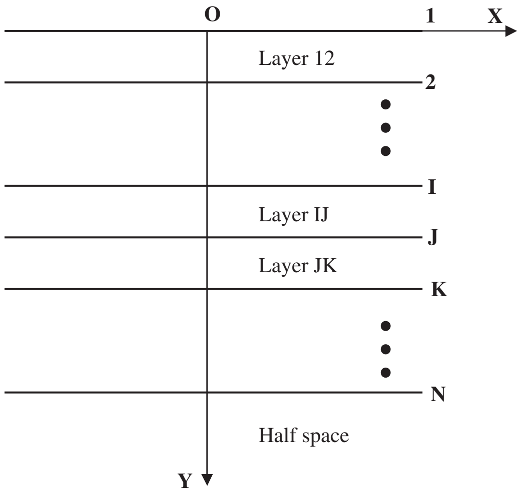

Fig. 1. ($N-1$) sublayers overlaying on a semi-infinite solid.

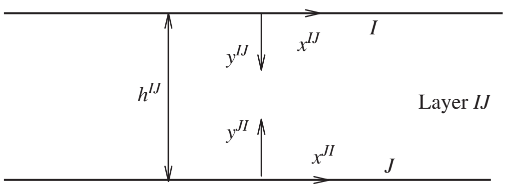

Fig. 2. Two local coordinate systems in each sublayer.

In the local Cartesian coordinate system $(x, y)^{IJ}$, the transformed wave equations associated with displacement potentials $\hat{\varphi}^{IJ}$ and $\hat{\psi}^{IJ}$ are denoted as

$$\frac{\partial^2 \hat{\varphi}^{IJ}}{\partial y^2} - (p\lambda_1^{IJ})^2 \hat{\varphi}^{IJ} = 0, \tag{2}$$

$$\frac{\partial^2 \hat{\psi}^{IJ}}{\partial y^2} - (p\lambda_2^{IJ})^2 \hat{\psi}^{IJ} = 0, \tag{3}$$

where

$$\lambda_1^{IJ} = \sqrt{(c^{IJ})^{-2} - \eta^2}, \quad \lambda_2^{IJ} = \sqrt{(C^{IJ})^{-2} - \eta^2}.$$

c^{IJ} and C^{IJ} are velocities of P and S waves of sublayer IJ, respectively. Correspondingly, the transformed displacement vector $\hat{\mathbf{U}}^{IJ}(\eta, y^{IJ}, p) = \{\hat{u}_x^{IJ}, \hat{u}_y^{IJ}\}^{\mathrm{T}}$ is expressed as

$$\hat{\mathbf{U}}^{IJ}(\eta, y^{IJ}, p) = p\mathbf{A}_u^{IJ}\hat{\mathbf{a}}^{IJ} + p\mathbf{D}_u^{IJ}\hat{\mathbf{d}}^{IJ}, \tag{4}$$

and the transformed stress vector $\hat{\mathbf{F}}^{IJ}(\eta, y^{IJ}, p) = \{\hat{\tau}_{yx}^{IJ}, \hat{\tau}_{yy}^{IJ}\}^{\mathrm{T}}$,

$$\hat{\mathbf{F}}^{IJ}(\eta, y^{IJ}, p) = \mu p^2\mathbf{A}_f^{IJ}\hat{\mathbf{a}}^{IJ} + \mu p^2\mathbf{D}_f^{IJ}\hat{\mathbf{d}}^{IJ}, \tag{5}$$

where $\hat{\mathbf{a}}^{IJ} = \{a_1^{IJ}, a_2^{IJ}\}^{\mathrm{T}}$ and $\hat{\mathbf{d}}^{IJ} = \{d_1^{IJ}, d_2^{IJ}\}^{\mathrm{T}}$ are unknown vectors, which represent wave–amplitude vectors of arriving and departing waves with respect to interface I in the local coordinate system $(x, y)^{IJ}$, respectively. $\mathbf{A}_u^{IJ}$ and $\mathbf{D}_u^{IJ}$ are phase-related receiver matrixes for displacements corresponding to arriving and departing waves in the local coordinate system $(x, y)^{IJ}$, respectively, which are denoted as the product of the receiver matrixes

$\bar{\mathbf{A}}_u^{IJ}$ and $\bar{\mathbf{D}}_u^{IJ}$, and phase matrixes $\mathbf{A}^{IJ}$ and $\mathbf{D}^{IJ}$

$$\mathbf{A}_u^{IJ} = \bar{\mathbf{A}}_u^{IJ}\mathbf{A}^{IJ} = \begin{bmatrix} \eta & \gamma_2^{IJ} \\ \gamma_1^{IJ} & -\eta \end{bmatrix} \begin{bmatrix} e^{p\gamma_1^{IJ}y^{IJ}} & 0 \\ 0 & e^{p\gamma_2^{IJ}y^{IJ}} \end{bmatrix}, \tag{6a}$$

$$\mathbf{D}_u^{IJ} = \bar{\mathbf{D}}_u^{IJ}\mathbf{D}^{IJ} = \begin{bmatrix} \eta & -\gamma_2^{IJ} \\ -\gamma_1^{IJ} & -\eta \end{bmatrix} \begin{bmatrix} e^{-p\gamma_1^{IJ}y^{IJ}} & 0 \\ 0 & e^{-p\gamma_2^{IJ}y^{IJ}} \end{bmatrix}. \tag{6b}$$

$\mathbf{A}_f^{IJ}$ and $\mathbf{D}_f^{IJ}$ are phase-related receiver matrixes for stresses corresponding to arriving and departing waves in the local coordinate system $(x, y)^{IJ}$, respectively, which are expressed as

$$\mathbf{A}_f^{IJ} = \bar{\mathbf{A}}_f^{IJ}\mathbf{A}^{IJ} = \begin{bmatrix} 2\eta\gamma_1^{IJ} & (\gamma_2^{IJ})^2 - \eta^2 \\ (\gamma_2^{IJ})^2 - \eta^2 & -2\eta\gamma_2^{IJ} \end{bmatrix} \begin{bmatrix} e^{p\gamma_1^{IJ}y^{IJ}} & 0 \\ 0 & e^{p\gamma_2^{IJ}y^{IJ}} \end{bmatrix}, \tag{7a}$$

$$\mathbf{D}_f^{IJ} = \bar{\mathbf{D}}_f^{IJ}\mathbf{D}^{IJ} = \begin{bmatrix} -2\eta\gamma_1^{IJ} & (\gamma_2^{IJ})^2 - \eta^2 \\ (\gamma_2^{IJ})^2 - \eta^2 & 2\eta\gamma_2^{IJ} \end{bmatrix} \begin{bmatrix} e^{-p\gamma_1^{IJ}y^{IJ}} & 0 \\ 0 & e^{-p\gamma_2^{IJ}y^{IJ}} \end{bmatrix}. \tag{7b}$$

In order to simplify the expressions in the following analysis, we arrange γ_1, γ_2, h, and y of all sublayers in the following sequence:

$$\{\gamma_1, \gamma_2, \ldots, \gamma_{2N-3}, \gamma_{2N-2}\} = \{\gamma_1^{12}, \gamma_2^{12}, \ldots, \gamma_1^{(N-1)N}, \gamma_2^{(N-1)N}\}, \tag{8a}$$

$$\{h_1, h_2, \ldots, h_{2N-3}, h_{2N-2}\} = \{h^{12}, h^{12}, \ldots, h^{(N-1)N}, h^{(N-1)N}\}, \tag{8b}$$

$$\{y_1, y_2, \ldots, y_{2N-3}, y_{2N-2}\} = \{y^{12}, y^{12}, \ldots, y^{(N-1)N}, y^{(N-1)N}\}. \tag{8c}$$

We define the arriving wave amplitude vector $\mathbf{a}^J$ and the departing wave amplitude vector $\mathbf{d}^J$ of interface J as

$$\mathbf{a}^J = \{a_1^{J(J-1)}, a_2^{J(J-1)}, a_1^{J(J+1)}, a_2^{J(J+1)}\}^{\mathrm{T}}, \tag{9a}$$

$$\mathbf{d}^J = \{d_1^{J(J-1)}, d_2^{J(J-1)}, d_1^{J(J+1)}, d_2^{J(J+1)}\}^{\mathrm{T}}. \tag{9b}$$

For the free surface, wave amplitude vectors will be revised as

$$\mathbf{a}^1 = \{a_1^{12}, a_2^{12}\}^{\mathrm{T}}, \tag{10a}$$

$$\mathbf{d}^1 = \{d_1^{12}, d_2^{12}\}^{\mathrm{T}}. \tag{10b}$$

The application of the boundary conditions yields the scattering relation at interface J

$$\mathbf{d}^J = \mathbf{S}^J\mathbf{a}^J + \mathbf{s}^J, \tag{11}$$

where $\mathbf{S}^J = -(\mathbf{D}^J)^{-1}\mathbf{A}^J$ and $\mathbf{s}^J = (\mathbf{D}^J)^{-1}\mathbf{F}^J(p)/p^2$ are the scattering matrix and the source matrix of interface J, respectively. $\mathbf{F}^J(p)$ is the external force vector of interface J. With the definition of the global arriving and departing wave amplitude vectors $\mathbf{a} = \{\{\mathbf{a}^1\}^{\mathrm{T}}, \{\mathbf{a}^2\}^{\mathrm{T}}, \ldots, \{\mathbf{a}^N\}^{\mathrm{T}}\}^{\mathrm{T}}$ and $\mathbf{d} = \{\{\mathbf{d}^1\}^{\mathrm{T}}, \{\mathbf{d}^2\}^{\mathrm{T}}, \ldots, \{\mathbf{d}^N\}^{\mathrm{T}}\}^{\mathrm{T}}$, the global scattering relation can be written in the following form

$$\mathbf{d} = \mathbf{S}\mathbf{a} + \mathbf{s}, \tag{12}$$

where

$$\mathbf{S} = \begin{bmatrix} \mathbf{S}^1 & & & \\ & \mathbf{S}^2 & & \\ & & \ddots & \\ & & & \mathbf{S}^N \end{bmatrix} \quad \text{and} \quad \mathbf{s} = \begin{bmatrix} \mathbf{s}^1 & & & \\ & \mathbf{s}^2 & & \\ & & \ddots & \\ & & & \mathbf{s}^N \end{bmatrix}$$

are the global scattering matrix and the global source matrix, respectively.

Since both vectors **a** and **d** are unknown quantities, we need an additional equation related to **a** and **d**. A wave arriving at interface I in the local coordinate $(x, y)^{IJ}$, is also considered as the wave departing from interface J of the same sublayer in the local coordinate $(x, y)^{IJ}$, which yields the other relation between the global arriving and departing wave amplitude vectors

$$\mathbf{a} = \mathbf{PHd}, \tag{13}$$

where the phase matrix **P** is a $(4N-2)\times(4N-2)$ diagonal matrix whose diagonal values are $\mathrm{e}^{-p\gamma_1 h_1}$,$-\mathrm{e}^{-p\gamma_2 h_2}$, $\mathrm{e}^{-p\gamma_1 h_1}$, $-\mathrm{e}^{-p\gamma_2 h_2},\ldots,\mathrm{e}^{-p\gamma_{2N-3}h_{2N-3}}$,$-\mathrm{e}^{-p\gamma_{2N-2}h_{2N-2}}$,$\mathrm{e}^{-p\gamma_{2N-3}h_{2N-3}}$,$-\mathrm{e}^{-p\gamma_{2N-2}h_{2N-2}}$, 0, 0. **H** is a $(4N-2)\times(4N-2)$ matrix composed of only one element whose value is one in each line and each row and others are all zero. For example, in vector **d**, if d_i^{JK} and d_i^{KJ} are in the positions p and q, respectively, then the elements H_{pq} and H_{qp} in the matrix **H** have the same value one.

Once the vectors **d** and **a** are known from Eqs. (12) and (13), the complete list of displacements in Laplace domain will be expressed as

$$\bar{\mathbf{U}}(x,y,p) = \frac{p^2}{2\pi\mathrm{i}}\int_{\eta_1-\mathrm{i}\infty}^{\eta_1+\mathrm{i}\infty}(\mathbf{A}_u\mathbf{PH}+\mathbf{D}_u)[\mathbf{I}-\mathbf{R}]^{-1}\mathbf{s}\mathrm{e}^{p\eta x}\mathrm{d}\,\eta, \tag{14}$$

where $\mathbf{R} = \mathbf{SPH}$ is the reverberation matrix. $\mathbf{A}_u$ and $\mathbf{D}_u$ are the global phase-related receiver matrixes for displacements corresponding to arriving and departing waves, respectively, which can be denoted as the product of the global receiver matrix and the global phase matrix,

$$\mathbf{A}_u = \bar{\mathbf{A}}_u\mathbf{A}, \tag{15a}$$

$$\mathbf{D}_u = \bar{\mathbf{D}}_u\mathbf{D}, \tag{15b}$$

where $\bar{\mathbf{A}}_u$ and $\bar{\mathbf{D}}_u$ are the global receiver matrixes. The global phase matrix **A** corresponding to arriving waves is a $(4N-2)\times(4N-2)$ diagonal matrix whose diagonal values are $\mathrm{e}^{p\gamma_1 y_1}$, $\mathrm{e}^{p\gamma_2 y_2}$, $\mathrm{e}^{p\gamma_1 y_1}$, $\mathrm{e}^{p\gamma_2 y_2},\ldots,\mathrm{e}^{p\gamma_{2N-3}y_{2N-3}}$, $\mathrm{e}^{p\gamma_{2N-2}y_{2N-2}}$, $\mathrm{e}^{p\gamma_{2N-3}y_{2N-3}}$, $\mathrm{e}^{p\gamma_{2N-2}y_{2N-2}}$, 0, 0. The global phase matrix **D** corresponding to departing waves is a $(4N-2)\times(4N-2)$ diagonal matrix whose diagonal values are $\mathrm{e}^{-p\gamma_1 y_1}$, $\mathrm{e}^{-p\gamma_2 y_2}$, $\mathrm{e}^{-p\gamma_1 y_1}$, $\mathrm{e}^{-p\gamma_2 y_2},\ldots,\mathrm{e}^{-p\gamma_{2N-3}y_{2N-3}}$, $\mathrm{e}^{-p\gamma_{2N-2}y_{2N-2}}$, $\mathrm{e}^{-p\gamma_{2N-3}y_{2N-3}}$, $\mathrm{e}^{-p\gamma_{2N-2}y_{2N-2}}$, 0, 0.

The replacement of the inverse of the matrix $\mathbf{I}-\mathbf{R}$ by a power series $[\mathbf{I}+\mathbf{R}+\mathbf{R}^2+\cdots+\mathbf{R}^n+\cdots]$ through the Neumann-expansion in Eq. (14) yields

$$\bar{\mathbf{U}}(x,y,p) = \frac{p^2}{2\pi\mathrm{i}}\sum_{n=0}^{\infty}\int_{\beta-\mathrm{i}\infty}^{\beta+\mathrm{i}\infty}(\mathbf{A}_u\mathbf{PH}+\mathbf{D}_u)\mathbf{R}^n\mathbf{s}\mathrm{e}^{p\eta x}\,\mathrm{d}\eta. \tag{16}$$

Here, each term in the above integral containing $\mathbf{R}^n$ are defined as a generalized-ray group, which represents the set of n times reflections and refractions of the source waves arriving at receivers at (x, y). The generalized-ray group with respect to $n = 0$ shows the waves from sources to the receivers directly, which are called as source waves. Here, every generalized-ray group contains a series of generalized rays, and the number of generalized rays increases exponentially with the increase of the number of sublayers and the reflection or refraction times.

The transient response of displacements can be denoted by the inverse Laplace transform of Eq. (16)

$$\mathbf{U}(x,y,t) = -\frac{1}{4\pi^2}\sum_{n=0}^{\infty}\int_{-\mathrm{i}\infty}^{+\mathrm{i}\infty}\int_{\beta-\mathrm{i}\infty}^{\beta+\mathrm{i}\infty}p^2\mathbf{G}_n\mathrm{e}^{p(\eta x+t)}\,\mathrm{d}\eta\,\mathrm{d}p, \tag{17}$$

where $\mathbf{G}_n(p,\eta) = (\mathbf{A}_u\mathbf{PH} + \mathbf{D}_u)\mathbf{R}^n\mathbf{s}$. Introducing the substitution $\eta = \xi/p$ in Eq. (17), Each of generalized-ray group integrals can be denoted as

$$\mathbf{U}_n(x,y,t) = -\frac{1}{4\pi^2}\int_{-\mathrm{i}\infty}^{+\mathrm{i}\infty}\int_{\beta-\mathrm{i}\infty}^{\beta+\mathrm{i}\infty} p\mathbf{G}_n(p,\xi/p)\mathrm{e}^{\xi x+pt}\,\mathrm{d}\xi\,\mathrm{d}p. \tag{18}$$

Considering finite x range $[-X/2, X/2]$ with K_1 sampling points and finite observation time range $[0, T]$ with M_1 sampling points, Eq. (18) was truncated, discretized, and numerically evaluated by FILT and FFT [12,13], which is expressed as

$$\mathbf{U}_n(lX/K_1, y, jT/M_1) = \frac{\mathrm{e}^{(\beta jT/M_1)+\mathrm{i}\pi l}}{TX}\sum_{m=0}^{m=M_1-1}\sum_{k=0}^{k=K_1-1}\mathbf{F}_n(m,k)W_1^{mj}W_2^{kl}, \tag{19}$$

where $l = 0,1,\ldots,K_1-1$ and $j = 0,1,\ldots,M_1-1$. $W_1 = \mathrm{e}^{-2\pi\mathrm{i}/M_1}$, $W_2 = \mathrm{e}^{-2\pi\mathrm{i}/K_1}$.

$$\mathbf{F}_n(m,k) = p_m\mathbf{G}_n(p_m, \xi_k/p_m),$$

$$\xi_k = -2\mathrm{i}\pi(k - K_1/2)/X,$$

$$p_m = \begin{cases} \beta - 2\pi\mathrm{i}m/T, & m = 0,1,\ldots,M_1/2 \\ \beta - 2\pi\mathrm{i}(m - M_1)/T, & m = M_1/2,\ldots,M_1-1 \end{cases}.$$

However, FILT–FFT algorithm shows high frequency oscillations near the discontinuities, known as Gibbs oscillations, which lead to amplitude errors that are unacceptable for the arrival-time determination of the generalized-ray groups. If no accurate arrival time of the generalized-ray groups, the Neumann-expansion truncation of $[\mathbf{I}-\mathbf{R}]^{-1}$ is difficult to be determined in finite observation time range $[0, T]$.

3. Expansion of generalized-ray group integrals

Each of generalized-ray groups contains a series of generalized rays with different arrival time. In order to determine the accurate arrival time of generalized-ray groups, each generalized-ray group integral must be expanded into the sum of a series of generalized rays, whose arrival time and responses can be accurately evaluated by Cagniard–De Hoop method. Each of generalized-ray integrals is constructed by assembling the source function, reflection and refraction coefficients, the receiver function, and the phase function. Except for the phase function, each of generalized-ray group integrals in Eq. (16) also has the source matrix $\mathbf{S}$, reflection and refraction matrix (reverberation matrix) $\mathbf{R}$, and receiver matrixes $\mathbf{A}_u\mathbf{P}$ and $\mathbf{D}_u$, which is similar with the generalized-ray integral. In order to expand a generalized-ray group integral into the sum of the generalized-ray integrals, the phase function $\mathrm{e}^{pg(\eta)}$ corresponding to the different generalized ray must be extracted from the generalized-ray group integrals.

Different from the generalized-ray integral, the phase function $\mathrm{e}^{pg(\eta)}$ in the generalized-ray group integral are involved in the receiver matrixes $\mathbf{A}_u\mathbf{P}$ and $\mathbf{D}_u$, and reverberation matrix $\mathbf{R}$. Firstly, we extract the phase function from the receiver matrix $\mathbf{A}_u\mathbf{P}$. For general case that there is only one receiver in each finite sublayer with a distance of y_j from the top surface of each sublayer, extraction of the phase function from $\mathbf{A}_u\mathbf{P}$ yields

$$\mathbf{A}_u\mathbf{P} = \sum_{j=1}^{2N-2}\bar{\mathbf{A}}_u\mathbf{A}_j\mathbf{P}_j\,\mathrm{e}^{pt_{aj}}, \tag{20}$$

where $\mathbf{A}_j$ is a $(4N-2)\times(4N-2)$ diagonal matrix with two nonzero elements whose values are ones at $(2j–1)$ and $(2j+1)$ for odd j, and $(2j–2)$ and $(2j)$ for even j. $\mathbf{P}_j$ is a $(4N-2)\times(4N-2)$ diagonal matrix with only two nonzero elements whose values are ones at $(2j–1)$ and $(2j+1)$ for odd j, and negative ones at $(2j–2)$ and $(2j)$ for even j. $t_{aj} = \gamma_j(y_j - h_j)$. If we only consider a receiver in Kth sublayer, Eq. (20) will be simplified into

$$\mathbf{A}_u\mathbf{P} = \sum_{j=2K-1}^{2K}\bar{\mathbf{A}}_u\mathbf{A}_j\mathbf{P}_j\,\mathrm{e}^{pt_{aj}}. \tag{21}$$

Similarly, $\mathbf{D}_u$ can be denoted as

$$\mathbf{D}_u = \sum_{j=1}^{2N-2} \bar{\mathbf{D}}_u \mathbf{D}_j \, \mathrm{e}^{-pt_{dj}}, \tag{22}$$

where $\mathbf{D}_j$ is a $(4N-2) \times (4N-2)$ diagonal matrix with two nonzero elements whose values are ones at $(2j-1)$ and $(2j+1)$ for odd j, and $(2j-2)$ and $(2j)$ for even j. $t_{dj} = \gamma_j y_j$.

Secondly, the nth power of reverberation matrix $\mathbf{R}^n$ can be denoted as

$$\mathbf{R}^n = \sum_{q+r+\cdots+v=n} \bar{\mathbf{P}}(n : q, r, \ldots, v)\mathrm{e}^{-pt_R}, \tag{23}$$

where $\bar{\mathbf{P}}(n; q, r, \ldots, v)$ is the sum of the set taking q matrixes $\mathbf{R}_1 = \mathbf{SP}_1\mathbf{H}$, r matrixes $\mathbf{R}_2 = \mathbf{SP}_2\mathbf{H}, \ldots,$ and v matrixes $\mathbf{R}_{2(N-1)} = \mathbf{SP}_{2(N-1)}\mathbf{H}$ to multiply in the sequence of permutation with repetition. For example, considering two matrixes $\mathbf{R}_1$ and one matrix $\mathbf{R}_2$, $\bar{\mathbf{P}}(3; 2, 1)$ equals $\mathbf{R}_1\mathbf{R}_1\mathbf{R}_2 + \mathbf{R}_1\mathbf{R}_2\mathbf{R}_1 + \mathbf{R}_2\mathbf{R}_1\mathbf{R}_1$. $t_R = q\gamma_1 h_1 + r\gamma_2 h_2 + \cdots + v\gamma_{2(N-1)} h_{2(N-1)}$.

Substitution of Eqs. (20), (22), and (23) into Eq. (16) results in the sum of a series of the generalized rays

$$\bar{\mathbf{U}}(x, y, p) = \sum_{n=0}^{\infty} \sum_{j=1}^{2N-2} \sum_{q+r+\cdots+v=n} \frac{1}{2\pi\mathrm{i}} \int_{\beta-\mathrm{i}\infty}^{\beta+\mathrm{i}\infty} (\mathbf{G}_a \mathbf{F}(p)\mathrm{e}^{-pt_1} + \mathbf{G}_d \mathbf{F}(p)\mathrm{e}^{-pt_2}) \, \mathrm{d}\eta, \tag{24}$$

where $\mathbf{G}_a = \mathbf{A}'_u \mathbf{A}_j \mathbf{P}_j \mathbf{H} \bar{\mathbf{P}}(n; q, r, \ldots, v)\mathbf{D}^{-1}$, $\mathbf{G}_d = \mathbf{D}'_u \mathbf{D}_j \bar{\mathbf{P}}(n; q, r, \ldots, v)\mathbf{D}^{-1}$, $t_1 = -\eta x + t_{aj} + t_R$, and $t_2 = -\eta x + t_{dj} + t_R$. The canonical form of each term in Eq. (24) can be denoted as

$$\bar{\mathbf{E}}(p) = \int_{\eta_1-\mathrm{i}\infty}^{\eta_1+\mathrm{i}\infty} \mathbf{G}(\eta)\mathrm{e}^{-pt} \, \mathrm{d}\eta \frac{\mathbf{F}(p)}{2\pi i}. \tag{25}$$

The inverse Laplace transform of the integral in Eq. (25) can be conducted by Cagniard–De Hoop method, which is shown in detail in the textbooks of Achenbach [16] and Pao [8]. The Cagniard–De Hoop scheme consists in deforming the path on integration in the η plane such that the integrals can be recognized as the Laplace transform of certain explicit functions of time. The inverse Laplace transform of the integral in Eq. (25) is shown as

$$\mathbf{E}(t) = \frac{1}{\pi} \mathrm{Im}\left\{ \mathbf{G}(\eta) \frac{\partial \eta}{\partial t} H(t - t_a) \right\}_{\eta=\eta_1} * L^{-1}\{\mathbf{F}(p)\}, \tag{26}$$

where $H(\cdot)$ is the Heaviside function, L^{-1} the inverse Laplace transform, and $*$ denotes the convolution of two functions with respect to time t. The deformed path of integration $\eta = \eta_1$ is given by the following equation:

$$t = -\eta x + t_{*j} + t_R, \tag{27}$$

where $t_{*j} = t_{aj}$ for arriving waves and $t_{*j} = t_{dj}$ for departing waves in Eq. (24). The arrival time t_a of each generalized ray is determined from the global stationary value of t, which is determined by the condition

$$\frac{\partial t}{\partial \eta} = 0. \tag{28}$$

If the arrival time t_a^{M-1} of the $(M-1)$th generalized-ray group is smaller than computational time length T and the arrival time t_a^M of the Mth generalized-ray group is greater than computational time length T, we only consider the sum of the first $(M-1)$ terms of the Neumann-expansion of $[\mathbf{I}-\mathbf{R}]^{-1}$ in the finite time range $[0, T]$.

4. Numerical results and discussion

We show two examples to verify the efficiency of the proposed method. The first is a sublayer overlaying a semi-infinite solid. The thickness of the sublayer is h_1, Lame constants $\lambda_1 = \mu_1$, and the density ρ_1. The Lame constants of the semi-infinite solid are $\lambda_2 = \mu_2 = 2\lambda_1$ and the density $\rho_2 = \rho_1$. A vertical line source

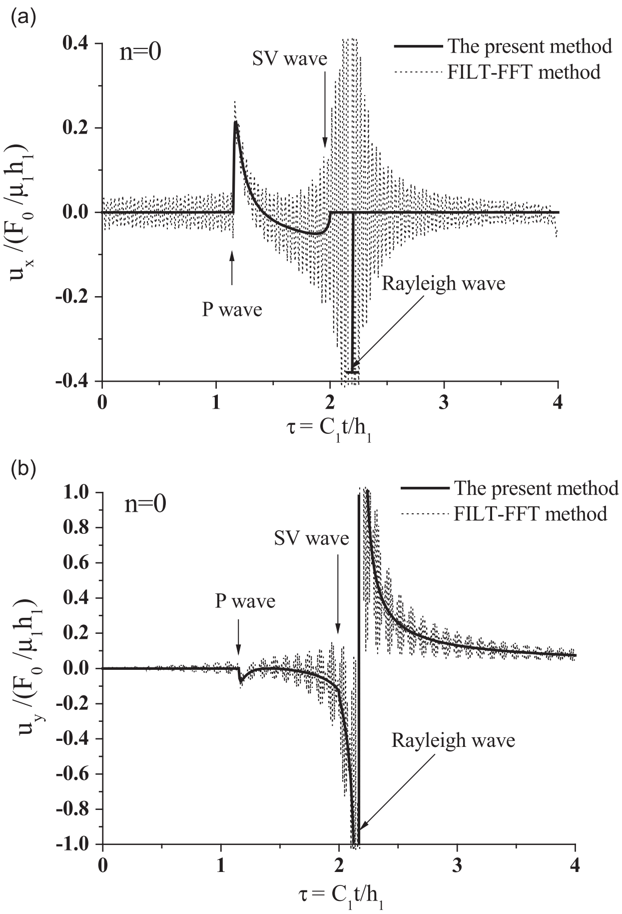

Fig. 3. The transient displacements of receiver A for the first generalized-ray group: (a) the horizontal displacement and (b) the vertical displacement.

$-F_0\delta(t)\delta(x)\delta(y)$ is acted on the free surface of the sublayer, and receivers A and B are also set at the free surface of the sublayer with the distance of $2h$ and $3h$ from the source, respectively.

Fig. 3 shows the transient displacements of receiver A for the first generalized-ray group calculated by Cagniard–De Hoop and FILT–FFT algorithms. Figs. 3(a) and (b) represent the horizontal and vertical displacements, respectively. In the following figures, the normalized displacements $u\mu_1 h_1/F_0$ and the normalized time $\tau = C_1 t/h$ are introduced. The first generalized-ray group includes the direct P wave, the direct S wave, and the Rayleigh wave, without any reflection or refraction from any interface of the multilayered solid. It is shown clearly that the arrival time of P wave, S wave, and Rayleigh wave calculated by Cagniard–De Hoop algorithm are $\tau = 2/\sqrt{3}$, 2, and 2.175, respectively, which are the same as results of Forrestal [17]. The horizontal displacement vanishes after the transverse wave has arrived, except for a δ-function propagating with the velocity of Rayleigh waves. The vertical displacement shows an infinite discontinuity propagating with the velocity of Rayleigh wave. Furthermore, the arrivals of P and S waves correspond to non-differentiability of the displacements. These non-differentiability and discontinuity of the displacements yield the high frequency oscillations of the results of FILT–FFT algorithm, which make it difficult to identify the arrival time of P wave, S wave, and Rayleigh wave for FILT–FFT algorithm.

The transient displacements of receiver A for the second generalized-ray group are shown in Fig. 4. The second generalized-ray group contains Pp, Ps, Sp, and Ss waves, which correspond to waves arriving at receiver A after reflection of source wave by the bottom interface of the finite sublayer. The arrival time of Pp

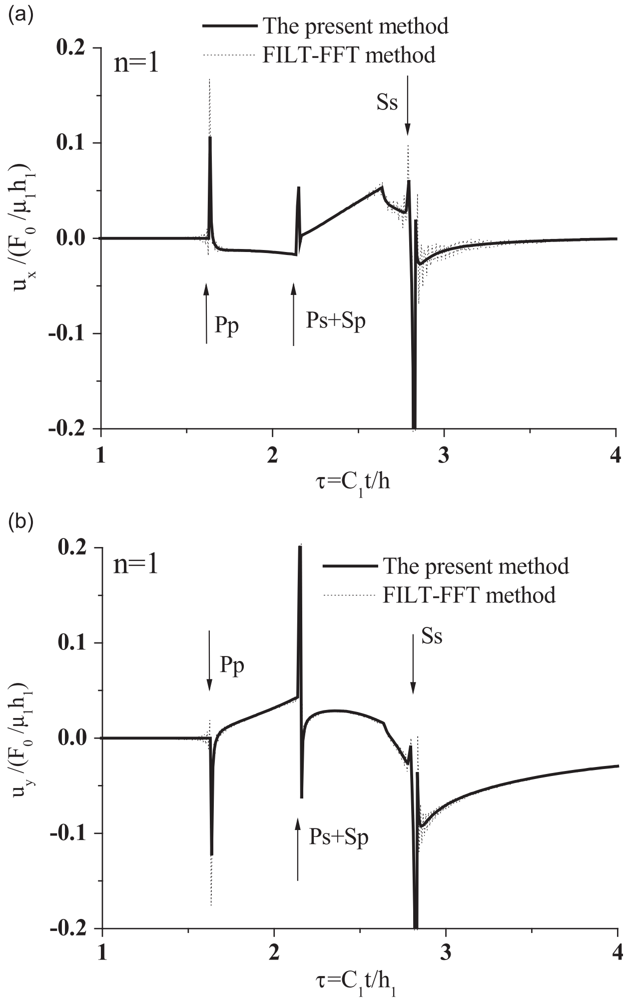

Fig. 4. The transient displacements of receiver A for the second generalized-ray group: (a) the horizontal displacement and (b) the vertical displacement.

wave is $\tau = 2\sqrt{2}/\sqrt{3}$, the arrival time of Ss wave $\tau = 2\sqrt{2}$ and the arrival time of Ps and Sp waves $\tau \approx 2.150$. Because of no influence of Rayleigh waves, the results of FILT–FFT algorithm is coincide with those of Cagniard–De Hoop algorithm, except for the small high-frequency oscillation near the arrival of waves.

According to computational time length $T = 4$ and the calculated arrival time of generalized-ray group, Neumann-expansion in Eq. (16) are truncated to be $n = 6$. The transient displacements of receiver A corresponding to the sum of the first seven ray groups are shown in Fig. 5. Because of free-surface reflection of the finite sublayer, the second and third generalized-ray groups arrive simultaneously, and the fourth and the fifth generalized-ray groups, the sixth and seventh generalized-ray groups as well. Compared with Figs. 3 and 4, the first three generalized-ray groups mainly contribute to the transient responses of receiver A.

In order to compare the calculation efficiency of Cagniard–De Hoop and FILT–FFT algorithms, time consumption for the calculation of the first seven generalized-ray groups of receiver A are listed in Table 1, with 512 sampling points in the finite time range [0, T]. For each generalized-ray group, it is shown that the time consumption of Cagniard–De Hoop algorithm is smaller than one fourteenth of that of FILT–FFT algorithm, which means that the proposed method is more efficient.

Fig. 6 shows the transient displacements of receiver B for the second generalized-ray group. For the first generalized-ray group, transient responses of receiver B are similar with those of receiver A, except for the

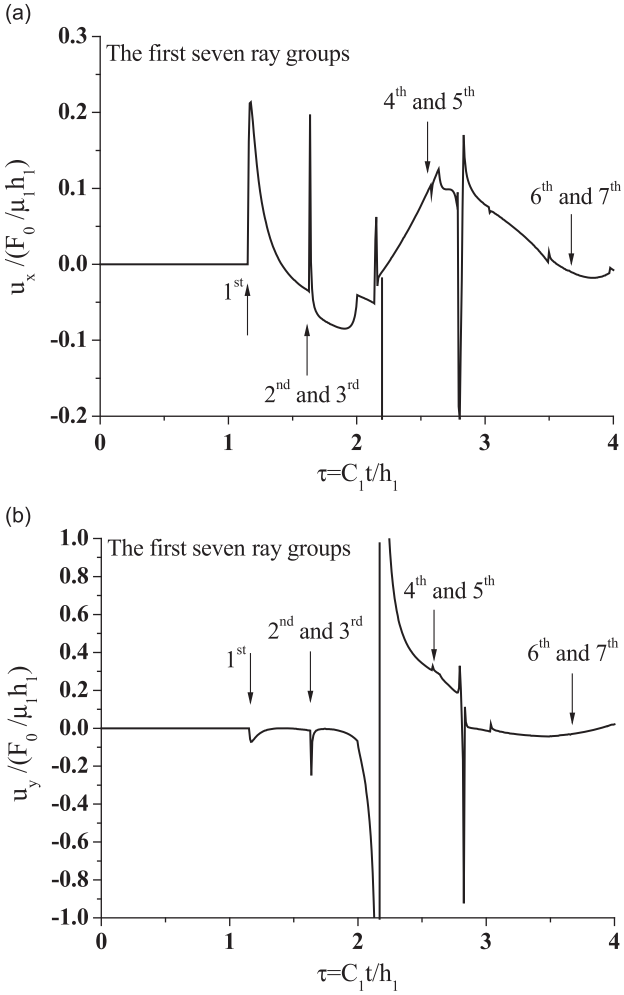

Fig. 5. The transient displacements of receiver A for the sum of the first seven generalized-ray groups: (a) the horizontal displacement and (b) the vertical displacement.

Table 1
Time consumption for the calculation of the generalized-ray groups of receiver A.

	Cagniard-De Hoop (s)	FILT–FFT (s)
The first generalized-ray group	19.27	692.80
The second generalized-ray group	39.83	696.12
The third generalized-ray group	43.43	699.16
The fourth generalized-ray group	35.26	703.21
The fifth generalized-ray group	21.87	705.21
The sixth generalized-ray group	10.96	706.20
The seventh generalized-ray group	5.20	707.92

arrival time of direct waves. Because the semi-infinite medium has higher wave velocities, the generalized rays may be refracted along the bottom interface of the finite sublayer. Fig. 6 shows clearly that three refracted waves PP*p, SP*p, and SS*s arrive at $\tau \approx 2.041$, 2.587, 3.536, respectively.

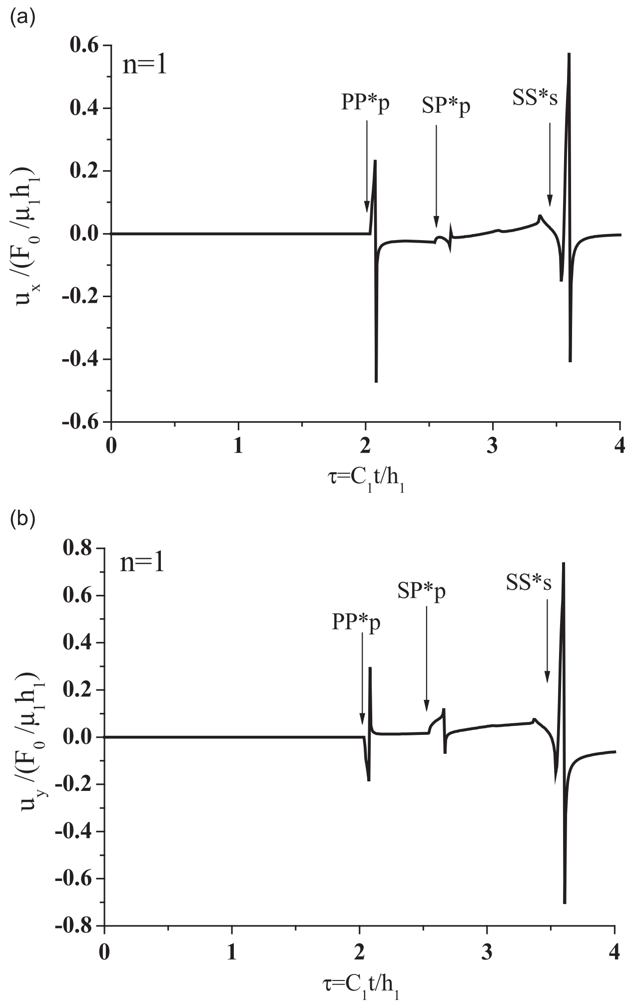

Fig. 6. The transient displacements of receiver B for the second generalized-ray group: (a) the horizontal displacement and (b) the vertical displacement.

The second example is four sublayers of the same thickness h_1 and density ρ overlaying a semi-infinite solid of density ρ. The first and third sublayers, and the semi-infinite solid have the same elastic constants with $\lambda_1 = \mu_1$, and Lame constants of the second and fourth sublayers double that of the first sublayer. The same source as the first example is applied on the free surface of the first sublayer. Receiver C is set in the semi-infinite solid with the horizontal distance of $5h$ from the source and a vertical distance of $0.5h$ from the top surface of the semi-infinite solid.

Fig. 7 shows the transient displacements of receiver C. Because receiver C is in the infinite solid, the waves from the source will arrive at receiver C directly after four times interface interaction ($n = 4$) so that the first four generalized-ray groups make no contribution to the response of receiver C. Considering this source–receiver configuration, only generalized-ray groups corresponding to the even of n contribute to the response of receiver C. The fifth ($n = 4$), seventh ($n = 6$), ninth ($n = 8$) generalized-ray groups and their sum are shown in Figs. 7(a) and (c), and their sums in Figs. 7(b) and (d). The fifth, seventh and ninth generalized-ray groups, which arrive at $\tau \approx 3.341.3.859$, 4.894, contains 32, 256, and 1152 generalized rays, respectively. With the increase of the reflection or refraction times, the number of the generalized rays contained in the generalized-ray group increases exponentially, which leads to the remarkable increase of the calculation-time consumption shown in Table 2. For the eleventh generalized-ray group, the insufficiency of the computer memory yields the failure of the calculation for Cagniard–De Hoop algorithm.

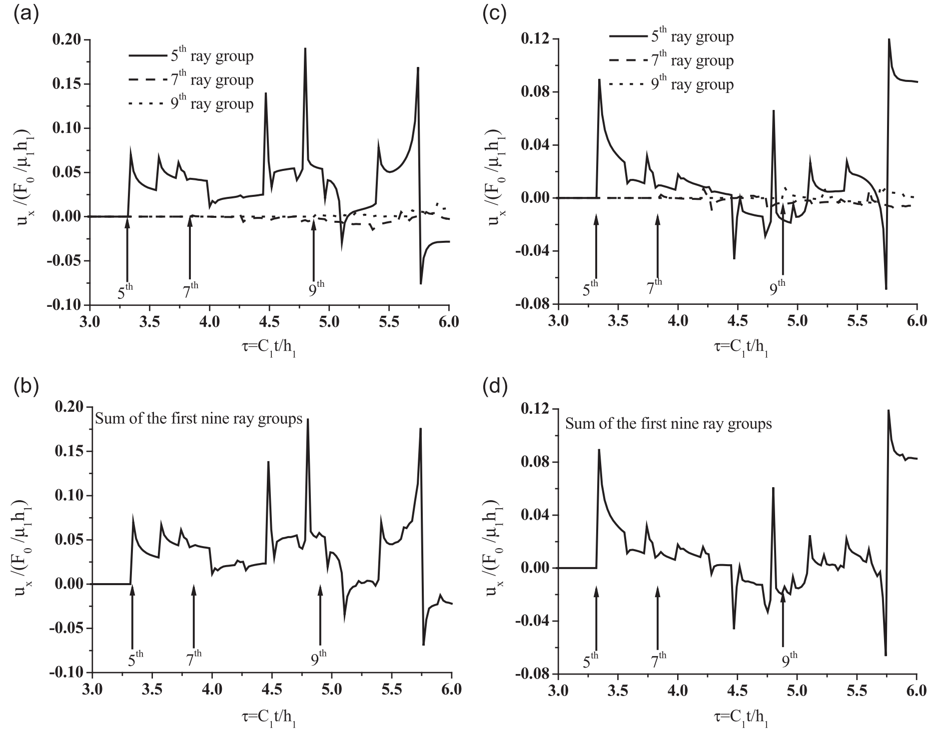

Fig. 7. The transient displacements of receiver C: (a) the fifth, seventh, and ninth generalized-ray groups for the horizontal displacement, (b) sum of the first nine generalized-ray groups for the horizontal displacement, (c) the fifth, seventh, and ninth generalized-ray groups for the vertical displacement, and (d) sum of the first nine generalized-ray groups for the vertical displacement.

Table 2
Time consumption for the calculation of the generalized-ray groups of receiver C.

	Cagniard-De Hoop (s)	FILT–FFT (s)
The fifth generalized-ray group	77.5	1474.5
The seventh generalized-ray group	953.6	1484.7
The ninth generalized-ray group	8243.8	1555.4

5. Conclusions

Combining reverberation matrix formulation with the theory of generalized rays, the hybrid method has been presented for the evaluation of the transient wave propagation in the multilayered solid. The combination of reverberation matrix formulation and Neumann-expansion expands the elastic waves in the multilayered solid into the sum of a series of the generalized-ray group integrals, which is suitable for the computer programming. Generalized-ray group integrals were evaluated numerically by FILT–FFT algorithm, which has the calculation burden and low precision. In order to calculate generalized-ray group integrals efficiently, extracting the phase function from the receiver matrixes and reverberation matrix yields a clear connection between the generalized-ray group integrals and the generalized-ray integrals, which can be accurately evaluated by Cagniard–De Hoop scheme in the theory of generalized rays. The numerical examples demonstrate that taking full advantage of automatic formulation of reflection or refraction coefficients of reverberation matrix method, and fast-high-precise calculation of generalized-ray method, this proposed method can calculate the arrival time and transient responses of the first several generalized-ray groups accurately in the complex multilayered-solid configuration with the lower time consumption, compared with FILT–FFT algorithm. However, with the times of reflection or refraction from interfaces, the number of generalized ray contained in the generalized-ray group will increase exponentially so that the insufficiency of the computer memory results in the failure of the long-time response calculation. Therefore, this proposed method will limit to the fast-high-precision analysis of early-time response in the complex multilayered-solid configuration.

Acknowledgments

A part of this study was supported by the National Natural Science Foundation of China (no. 10602053 and no. 50808170), research grants from Institute of Crustal Dynamics (no. ZDJ2007-2) and for oversea-returned scholar, Personnel Ministry of China. We very much appreciate the critical review and valuable comments from anonymous reviewers.

References

[1] J.E. White, *Seismic Waves: Radiation, Transmission, and Attenuation*, McGraw-Hill, New York, 1965.
[2] T. Thomson, Transmission of elastic waves through a stratified solid medium, *Journal of Applied Physics* 21 (2) (1950) 89–93.
[3] N.A. Haskell, The dispersion of surface waves on multi-layered media, *Bulletin of the Seismological Society of America* 43 (1953) 17–34.
[4] L. Wang, S.I. Rokhlin, Stable reformulation of transfer matrix method for wave propagation in layered anisotropic media, *Ultrasonics* 39 (2001) 413–424.
[5] S.I. Rokhlin, L. Wang, Stable recursive algorithm for elastic wave propagation in layered anisotropic media: Stiffness matrix method, *The Journal of the Acoustical Society of America* 112 (2002) 822–834.
[6] M. Lowe, Matrix techniques for modeling ultrasonic waves in stratified media, *IEEE Transactions on Ultrasonics, Ferroelectrics and Frequency Control* 42 (4) (1995) 525–542.
[7] T.W. Spencer, The method of generalized reflection and transmission coefficients, *Geophysics* 25 (1960) 625–641.
[8] Y.H. Pao, R.R. Gajewski, The generalized ray theory and transient responses of layered elastic solids, *Physics Acoustics*, Vol. 13, Academic Press, New York, 1977, pp. 183–265.
[9] G.S. Lee, C.C. Ma, Transient elastic waves propagating in a stratified medium subjected to in-plane dynamic loadings—part I: theory, *Proceedings of the Royal Society of London, Series A* 456 (2000) 1355–1374.
[10] C.C. Ma, G.S. Lee, Transient elastic waves propagating in a stratified medium subjected to inplane dynamic loadings—part II: numerical calculation and experimental measurement, *Proceedings of the Royal Society of London, Series A* 456 (2000) 1375–1396.
[11] C.C. Ma, G.S. Lee, General three-dimensional analysis of transient elastic waves in multilayered medium, *ASME Journal of Applied Mechanics* 73 (2) (2006) 490–504.
[12] X.Y. Su, J. Tian, Y.H. Pao, Application of reverberation-ray matrix to the propagation of elastic waves in a multi-layered solid, *International Journal of Solids and Structures* 39 (2002) 5447–5463.
[13] J. Tian, W.X. Yang, X.Y. Su, Transient elastic waves in a transversely isotropic laminate impacted by axisymmetric load, *Journal of Sound and Vibration* 289 (2006) 94–108.
[14] S.M. Howard, Y.H. Pao, Analysis and experiment on stress waves in planar trusses, *ASCE Journal of Engineering Mechanics* 128 (1998) 854–891.
[15] Y.H. Pao, W.Q. Chen, X.Y. Su, The reverberation-ray matrix and transfer matrix analysis, *Wave Motion* 44 (2007) 419–438.
[16] J.D. Achenbach, *Wave Propagation in Elastic Solids*, North-Holland, Amsterdam, 1973.
[17] M.J. Forrestal, L.E. Fugelso, G.L. Neidhardt, R.A. Felder, Response of a half space to transient loads, *Proceedings of the ASCE Engineering Mechanics Division Specialty Conference* (1966) 719–751.